Biochemical and Biophysical Research Communications 422 (2012) 405–410

Contents lists available at SciVerse ScienceDirect

Biochemical and Biophysical Research Communications

journal homepage: www.elsevier.com/locate/ybbrc

# Identification of microRNA–RNA interactions using tethered RNAs and streptavidin aptamers

Huan Liu, Siyuan Zhang, Heng Lin, Rong Jia, Zhi Chen *

*State Key Laboratory Breeding Base of Basic Science of Stomatology (Hubei-MOST) and Key Laboratory for Oral Biomedicine of Ministry of Education (KLOBM), School and Hospital of Stomatology, Wuhan University, Wuhan 430079, China*

ARTICLE INFO

*Article history:*
Received 23 April 2012
Available online 7 May 2012

*Keywords:*
Tethered RNAs
Streptavidin aptamers
miRNA pull-down

ABSTRACT

The molecular mechanisms of cell differentiation, organogenesis and tumorigenesis are directed by the gene regulatory network (GRN). Genes regulating all of these events are primarily post-transcriptionally inhibited by microRNAs (miRNAs), which are short non-coding RNAs that function mainly via binding to the 3′ untranslated regions (3′UTRs) of the target mRNAs. Identification of the miRNAs that bind to the genes in the GRN is crucial for understanding the GRN at the transcriptional level. Previously reported biomedical methods of identification for miRNA–RNA interactions primarily focused on the miRNA response elements (MRE) within the target RNA sequences, but the cognate miRNAs cannot identify all the miRNAs regulating a single target gene and cannot be used for *in vivo* experiments. In this study, we report a novel and efficient way to identify miRNAs that bind to a specific RNA sequence utilizing tethered RNA and streptavidin aptamers, which were previously employed for protein–RNA interaction research. We developed an optimized RNA pull-down assay with a combination of UV-crosslinking, streptavidin aptamers and magnetic beads, and with this method we identified the miRNAs binding to the 3′UTR of krüpple-like factor 4 (KLF4) in mouse dental papilla cells, as predicted by bioinformatic analysis, as well as the enrichment of the members in the let-7 miRNA family in the same cells. Furthermore, we developed an optimized method for the staining of streptavidin aptamers *in vivo*. Our method, which takes advantage of RNA aptamers, can be a powerful tool for direct and high-throughput identification of all of the miRNAs interacting with the target RNAs.



## 1. Introduction

The gene regulatory network (GRN) is a collection of genes in a cell, an organ or a living creature that interact with each other directly or indirectly, thereby governing the rates at which genes are transcribed into mRNA [1]. The study of the GRN has shed new light on the understanding of multiple biological processes such as cell differentiation, tumorigenesis and organogenesis. MicroRNAs (miRNAs) are short, non-coding regulatory RNAs involved in numerous types of biological events in which they post-transcriptionally inhibit gene expression via binding to partially or perfectly complementary sequences in the target mRNA [2–4]. Identification of the miRNAs interacting with their target genes may extend the understanding of the GRN at the post-transcriptional level, thus enhancing our knowledge of the mechanisms of the regulation of biological processes. Therefore, many bioinformatic approaches have been developed to predict the targets of miRNAs, as well as the binding of miRNAs to specific target sequences that are evolutionarily conserved across species, based on the tendency of miRNAs to form complete base pairings to the target mRNA at miRNA nucleotides 2–8 (the seed region) [5]. However, confirmation of the *in silico* assay results is difficult. To identify the targets of a specific miRNA, RNA immunoprecipitation chip (RIP-chip) [6,7], high-throughput sequencing of RNAs (HITS-CLIP) [8] and photoactivatable-ribonucleoside-enhanced crosslinking and immunoprecipitation (PAR-CLIP) [9] were sequentially developed, elegantly combining immunoprecipitation of the units in an miRNA–ribonucleoprotein complex with mRNA microarray and RNA-sequencing methods. However, these methods, empirically based on the direct effect of the overexpression of one miRNA, cannot rule out an indirect effect of this miRNA on other miRNAs, thus increasing the possibility of false positive hits. On the other hand, to identify the miRNAs interacting with target RNA sequences, the traditional dual luciferase assay and a biotinylated synthetic microRNA pull-down experiment [10] can only identify a microRNA binding to one target sequence at a time. Moreover, these methods rely heavily on synthetic oligoribonucleotides, which are usually expensive and often have a low affinity for target mRNA.

Previously, RNA aptamers have been proven to be potential ideal RNA tags for the detection of RNA–protein interactions and the affinity purification of RNPs [11]. In the presence of $Mg^{2+}$, tRNAs fold into stable clover-leaf structures that are resistant to

* Corresponding author. Fax: +86 27 87686198.
*E-mail address:* zhichen@whu.edu.cn (Z. Chen).

0006-291X/$ - see front matter © 2012 Elsevier Inc. All rights reserved.
http://dx.doi.org/10.1016/j.bbrc.2012.05.002

unfolding and can protect RNA fusions from degradation [12,13]. Recently, Macra developed an efficient method by the combination of streptavidin aptamers and tRNA structures, making the identification of the proteins binding to RNA simple and straightforward [12]. Thus, given the mechanism of miRNA–mRNA interactions, we reasoned that tRNA could serve as a useful scaffold for the affinity purification of the miRNA–mRNA complex, as well as for the detection of the miRNA–mRNA interaction.

In this report, we adopted the combination of tRNA and streptavidin aptamers to describe a robust and efficient approach to identify the miRNAs that bind to a specific RNA sequence, along with possible applications of this method.

## 2. Material and methods

### 2.1. Cell culture and transfection

Following a previously published protocol [14], the dental papilla mesenchymal cells were isolated from the first lower molars of E18.5 Swiss mice, after the approval from the Wuhan University Animal Ethic Committee, and digested for 1 h at 37 °C in a solution of 3 mg/mL collagenase type I and 4 mg/mL of dispase (Invitrogen, USA). The primary cultured mouse dental mesenchymal cells and the human embryonic kidney cell line 293FT were maintained in DMEM (Hyclone, USA) with 10% fetal bovine serum (Invitrogen, USA) and Antibiotic–Antimycotic (Invitrogen, USA) in a humidified 5% $CO_2$ atmosphere at 37 °C. Plasmids were transiently transfected into 293FT cells with X-tremeGENE HP DNA Transfection Reagent (Roche, Germany).

### 2.2. Plasmid construction

The 3′UTRs of mouse E2F1 and KLF4 were generated using PCR with the primers described in Table S1. The let-7 sponge was synthesized with 7 tandemly arrayed let-7 microRNA family seed sequences (methods as previously described [15]). All the DNA fragments were ligated into the EcoRI site of pcDNA3-tRSA or pcDNA-6×SA (kind gifts from Dr. Macara). The two binding sites of miR-20 within the 3′UTR were mutated using overlapping PCR. The tRSA-KLF4 3′UTR and the let-7 sponge fragment were subcloned into pLL3.7 (Addgene plasmid 11795), replacing the GFP coding sequence of the original plasmid. For the dual luciferase assay, the wildtype and mutant 3′UTR of E2F1 were subcloned into the pMIR-Reporter respectively.

### 2.3. Lentivirus production and transduction

All of the lentivectors were co-transfected with psPAX2 and pMD2.G (kind gifts from Dr. Trono) as described previously [16]. At 48 and 72 h after each co-transfection, the culture medium was collected then incubated with the 293FT cell line in the presence of Protamine (8 μg/mL; Sigma, USA) for titration. Mouse dental papilla mesenchymal cells were infected with the lentiviruses using the same multiplicity of infection (MOI = 7).

### 2.4. Tethered RNA streptavidin aptamer staining

$MgCl_2$ (10 mM) was included in all of the solutions used in this method, and the experiment was performed at room temperature. Cells growing on slides were fixed with 4% paraformaldehyde for 10 min, washed three times with PBS, and blocked with 0.3% $H_2O_2$ for 10 min followed by three washes with PBS. The slides were then incubated with streptavidin–HRP (Beyotime, China), washed with PBS three times, incubated with DAB for 20 s, and finally counterstained with methyl green (Beyotime, China).

### 2.5. miRNA pull-down assay

A schematic of the method is shown in the graphical abstract (Fig. 1). Cells were plated in 10 cm tissue culture dishes, transfected with 20 μg of plasmid, rinsed with PBS and then subjected to crosslinking at 400 mJ/cm$^2$ in a Strata linker. The cells were collected in 1 mL PBS with a cell scraper followed by resuspension in 1 mL lysis buffer (1× tissue culture-grade PBS, 1% NP-40, 0.25% deoxycholate, 10 mM $MgCl_2$, protease inhibitors and 200 U/mL RNasin (Promega, USA)). After a light sonication, the total cell lysates were placed on ice immediately. The pre-cleared lysates (300 μL) were mixed with 100% ethanol (450 μL) and applied to an RNeasy Mini column (QIAGEN, USA) to purify the RNA. At the same time, 200 μL of SA-PMPs (Promega, USA) were washed sequentially with 100 μL of nuclease-free 0.5× SSC (Ambion, USA), 100 μL of lysis buffer and 50 μL of lysis buffer using a magnetic stand. The pre-cleared lysates (300 μL) were applied to the prepared SA-PMPs. After incubation at 4 °C with mild rotation for 1 h, the SA-PMPs were washed with fresh lysis buffer followed by the addition of 700 μL of QIAzol, and the microRNAs were then isolated with the miReasy Mini Kit. To assay the enrichment of the pulled-down miRNAs, cDNA synthesis was performed with the miSript Reverse Transcription Kit (QIAGEN, USA), and real-time PCR was carried out using the ABI PRISM 7500 real-time PCR System (Applied Biosystems, USA) with a miScript Primer Assay set (Qiagen, USA) and a miScript SYBR Green PCR Kit (Qiagen, USA). The U6 snRNA level was used as an internal normalization control. Relative miRNA expression levels of the pull-down were normalized to those of the input, for which the cleared lysate was used. For confirmation of the transfection efficiency, RNA was isolated from 300 μL of pre-cleared lysates using the RNeasy mini kit and reverse transcribed with the SuperScript™ III First-Strand Synthesis System (Invitrogen, USA) for RT-PCR. GAPDH was employed as an internal normalization control. All the primer pairs are listed in Table S1.

### 2.6. Dual luciferase assay

A Renilla luciferase expression construct (phRL-TK; Promega, USA) was used as an internal control. Luciferase reporter plasmids with wildtype or mutant 3′UTR (1500 ng/well in a 6-well plate) along with phRL-TK (30 ng/well) were co-transfected into 293FT cells at 24 h post-transfection with the miRNA mimics (20 nM/well; GenePharma, China). Twenty-four hours later, the cells were harvested and lysed with passive lysis buffer (Promega, USA). Luciferase activity was measured by the Dual Luciferase Assay system (Promega, USA) following the manufacturer's instructions. The luminescence intensity of Firefly luciferase was normalized to that of Renilla luciferase.

### 2.7. Statistical analysis

Student's *t*-test was used, and $p < 0.05$ was considered significantly different. The results are displayed as the mean ± SEM from a minimum of three experiments for each experimental group.

## 3. Results

### 3.1. The tRSA tag and UV crosslinking improve the efficiency of the microRNA pull-down assay

At the beginning of the experiment, we generated the pcDNA3-6×SA plasmid by ligating the 3′UTR of E2F1 to the 3′-end of the six tandemly repeated aptamers. However, the miRNA pull-down assay did not yield a significantly different enrichment of miR-20

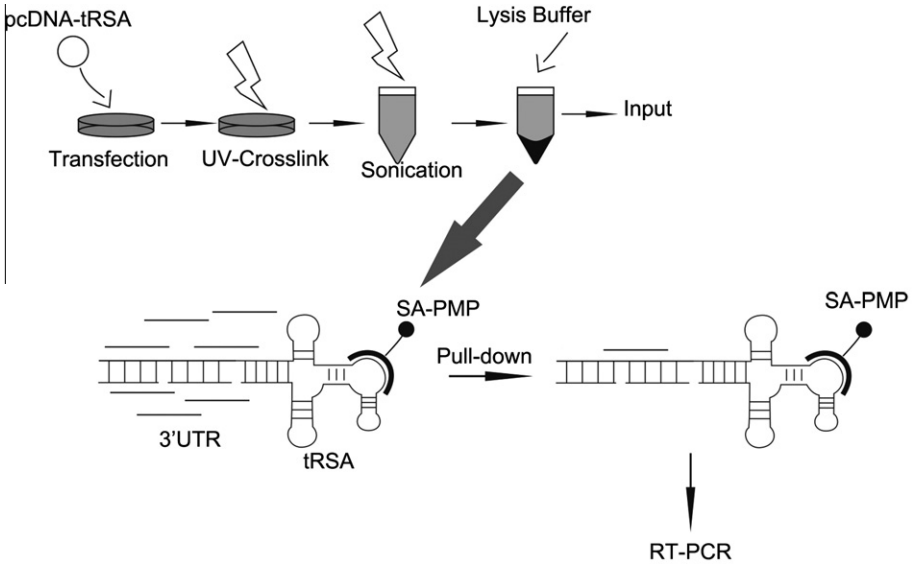


**Fig. 1.** Schematic of the procedure for miRNA pull-down with tRSA.

(Fig. 2A), which was previously shown to bind to the 3′UTR of E2F1 in 293FT cells. To improve the efficiency of the pull-down assay, we employed two strategies. First, we used the pcDNA3-tRSA plasmid by reasoning that the tethered structure of the RNA could stabilize the aptamer structure to facilitate the recognition of its targets. Second, because the formation of the miRNA–mRNA structure needs assistance from multiple types of proteins, we performed UV crosslinking before sonication to stabilize the ribonucleotide protein complex in the subsequent procedure.

As expected, compared with the relative miR-20 expression in each input group, both of these strategies improve the efficiency of miRNA enrichment, particularly the pull-down assay with UV crosslinking and tRSA structure, which can significantly enrich more miR-20 than any other combination of strategies ($p < 0.01$) (Fig. 2A). However, the 3′UTR of E2F1 with the mutant binding sites for miR-20 cannot bind miR-20 compared with the mock control (pcDNA3-tRSA). Dual-luciferase assays, as a traditional method, were performed to confirm the results (Fig. 2B).

### 3.2. The transfection efficiency of the RSA plasmids was revealed by biotin

To determine the transfection efficiency of the tRSA plasmids, we employed RT-PCR using the pre-cleared lysates before the miRNA pull-down experiments (Figs. 1 and 3). Additionally, because tRSA can bind to streptavidin, showing a similar behavior to biotin, we hypothesized that the transfection of tRSA could be revealed by a biotin staining method.

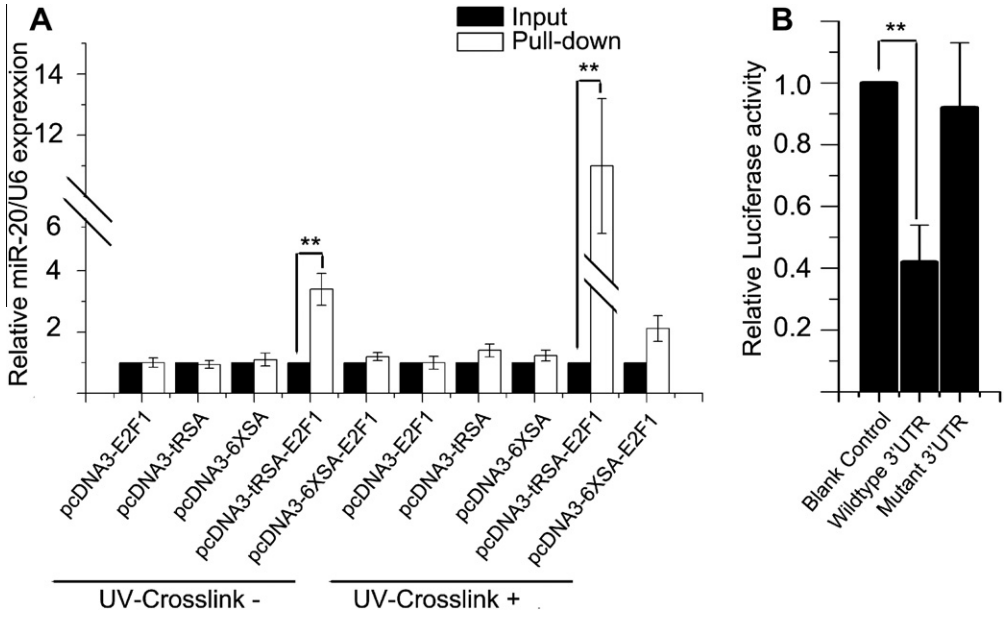


**Fig. 2.** The tRSA tag and UV crosslinking improve the efficiency of microRNA pull-down assays. (A) Real-time PCR analysis of the results from miRNA pull-down assays of different designs. The miRNA pull-down assays were tested using miR-20 and its validated target, E2F1. The binding to the 3′UTRs of 6×SA and tRSA were compared. 293FT cells were transfected with plasmids with different tags, and the lysates were used for the miRNA pull-down assay. UV crosslinking, when applied, was performed before sonication. UV-crosslinking combined with the tRSA tag gave the best outcome. (B) Dual luciferase validation for miR-20 interacting with E2F1. Two miR-20 binding sites within the cloned 3′UTR of E2F1 were mutated. Asterisks indicate statistical significance compared with the input groups: $^{*}p < 0.05$, $^{**}p < 0.01$.

First, we tested whether the binding of tRSA to the streptavidin beads could be blocked by biotin. Before applying the lysates to the SA-PMMs in the microRNA pull-down assay, the beads were incubated with biotin (2 mM in 0.5× SSC) for two hours (biotin group), while SA-PMPs incubated in 0.5× SSC were used as a control. The results showed that compared with the control group, the miR-20 pulled down in the biotin group was significantly less. This result not only indicated that the binding sites for streptavidin aptamer could be saturated by biotin but also implied that the tRSA RNA structure might be revealed by biotin. Additionally, the 293FT cells transfected with tRSA could be revealed using this procedure, while the 293FT cells transfected with pcDNA3 failed to give a positive signal (Fig. 3C and D).

### *3.3. The tRSA tag is capable of detecting miRNA binding to the 3′UTR primary transcript and the enrichment of miRNAs within the same microRNA family*

To evaluate the application of the tRSA system in detecting the miRNA–mRNA interaction, we chose the 3′UTR of KLF4 to detect microRNA binding. Additionally, taking advantage of the microRNA sponge and the tRSA, we employed the sponge for the let-7 microRNA family to determine the enrichment of microRNAs for the same family.

*In silico assays* using TargetScan and RNA22 predict that the miR-200c, miR-1a, miR-26a, miR-145, miR-135, miR-29, miR-146, miR-107, let-7a, miR-363, miR-128, miR-137 and miR-375 can bind to the 3′UTR of KLF4. Thus, we constructed a lentivector encoding the tRSA-3′UTR of KLF4 (tRSA-KLF4 group) and the tRSA (tRSA group) and then infected the primary-culture mouse dental papilla cells with the two lentiviruses. After infection, an miRNA pull-down assay was performed, and we detected that miR-200c, miR-1a, miR-26a, miR-145, miR-135, miR-29, miR-146, miR-363, miR-128, miR-137 and miR-375 were enriched by the 3′UTR of KLF4 compared with each relative input group (Fig. 4A). MiR-143 served as a negative control.

We recently found that the expression levels of let-7c decrease dramatically with the differentiation of odontoblasts (unpublished data). However, it has been hypothesized that with the same seed sequence, microRNAs in the same microRNA family share a similar function and expression level. Thus, we infected the dental papilla cells with the lentivirus coding the tRSA-tagged sponge for the let-7 miRNA family, and microRNA pull-down assays were performed. The results showed that seven members out of the let-7 microRNA family were detected (Fig. 4B).

## 4. Discussion

Studies of the gene regulatory network have demonstrated that numerous kinds of biological processes, such as tumorigenesis, organogenesis and cell differentiation, are orchestrated by several important genes termed hubs [1]. Thus, it is vital to investigate the miRNAs directly interacting with these hub genes. However, traditional studies on miRNAs mainly focus on a specific miRNA or a specific target. Here, we designed the bait RNA with a potential miRNA binding sequence using an tRSA tag that had been previously employed for the detection of RNA–RNP interactions [12]. Using this bait RNA structure, we successfully demonstrated the

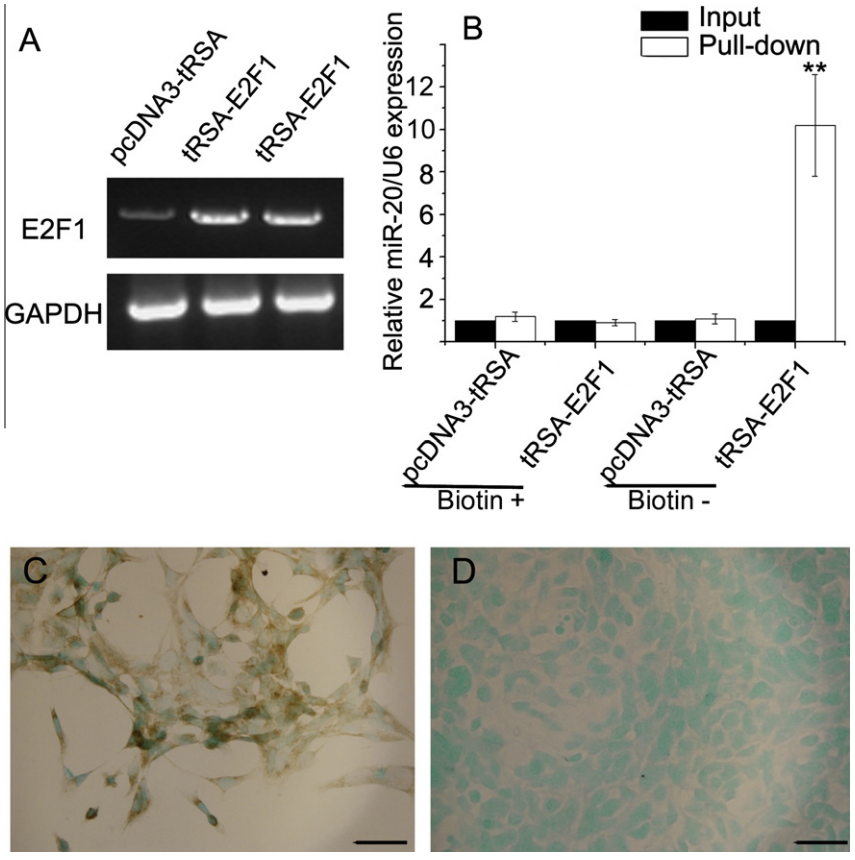


**Fig. 3.** The transfection efficiency of the tRSA plasmids could be revealed by biotin. (A) RT-PCR analysis of the transfection efficiency of the tRSA plasmids. The pre-cleared lysates from 293FT cells transfected with pcDNA3-tRSA or pcDNA3-tRSA-E2F1 were tested. (B) Real-time PCR analysis showed that biotin can block the binding of tRSA to SA-PMPs. Asterisks indicate statistical significance compared with the input groups: $^{*}p < 0.05$, $^{**}p < 0.01$. (C) 293FT cells transfected with pcDNA3-tRSA were stained. (D) 293FT cells transfected with pcDNA3 were stained with the same methods. Scale bars: (C and D), 100 μm.

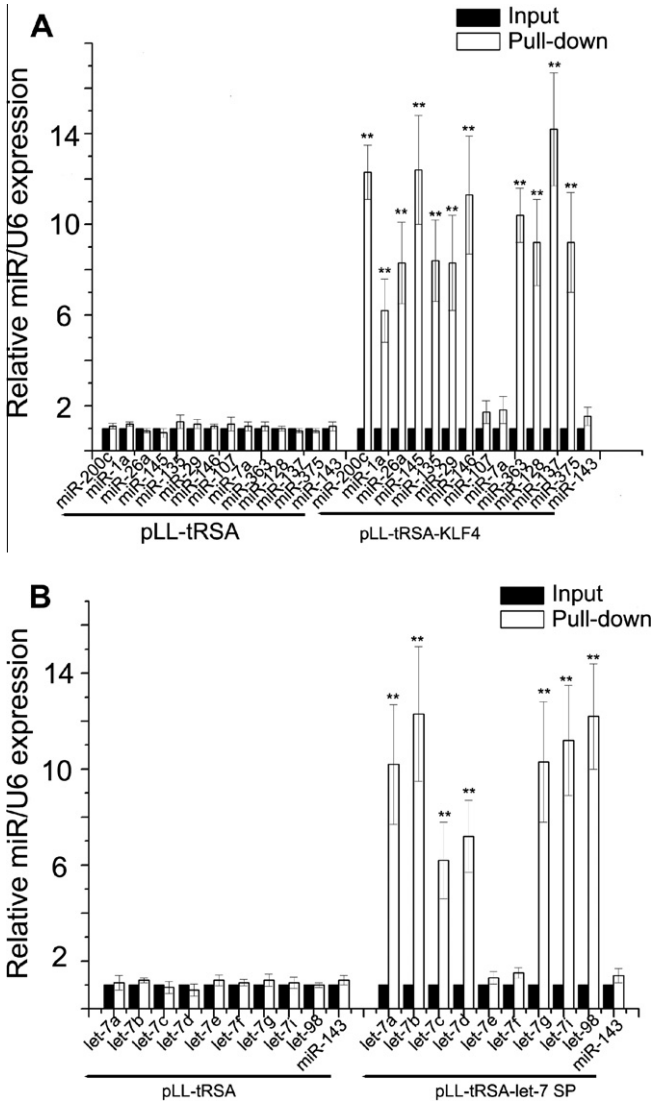


**Fig. 4.** Applications of the miRNA pull-down assay in detecting miRNA binding to a specific RNA sequence. Pull-down assays were performed on the lysates from cultures of primary mouse dental papilla cells using the 3′UTR of KLF4 (A) or the sponge for the let-7 miRNA family (B) as baits. Asterisks indicate statistical significance compared with the input groups: $^{*}p < 0.05$, $^{**}p < 0.01$.

identification of previously validated miRNAs, along with some novel miRNA–mRNA interactions. Additionally, we developed an optimized method to reveal tRSA within the cells. Lastly, we combined the miRNA sponge and tRSA to investigate the enrichment of the members in the let-7 miRNA family in mouse dental papilla cells.

Previously, RIP-ChIP and RISCome analyzes were developed sequentially to identify the target genes for a single miRNA, based on the results from microarray analysis following the immunoprecipitation of proteins in miRNA ribonucleoprotein complexes such as Ago2 and GW182 [7]. Furthermore, HITS-CLIP [6] and its improved version, PAR-CLIP [8], which elegantly combined immunoprecipitation and high-throughput RNA sequencing, detect miRNA targets at a higher resolution with a lower false positive rate. All of these methods, which focus on investigating the targets of a single miRNA and rely heavily on the transient transfection of labeled miRNAs, which has restricted studies to the cellular level, nonetheless identified potential MREs that must be tested subsequently with their cognate miRNAs. However, the approach reported in our study attempted to identify the interacting miRNAs themselves; also, the stably expressed tagged-bait RNA made it possible to shift the target identification experiment from the cell to the animal. In this report, we predicted the miRNAs that might bind to the 3′UTR of KLF4 with a bioinformatic approach and confirmed these predictions with real-time PCR using the primers for all of the candidate miRNAs. Ideally, high-throughput sequencing or microarray analysis could be employed to compare the enrichment of miRNAs in the 'pull-down' and 'input', thereafter determining all of the miRNAs interacting with the target RNA sequence.

One major obstacle in this method is normalization. Similar to the chromatin immunoprecipitation (ChIP) experiment design, we chose pre-cleared lysates as 'input' and compared the enrichment of miRNAs between 'input' and 'pull-down'. Because the relative expression level of U6 served as the internal control and would not be affected by the transfection and the subsequent washes, an increase in the relative expression level of miRNAs would indicate the enrichment of miRNAs by the pull-down assay, thereby demonstrating the binding of miRNAs to the bait RNA.

Furthermore, to develop a convenient way to detect the tRSA in transfected cells, we stained tRSA with a modified method previously for biotin, because tRSA can bind to streptavidin, competing with biotin. Our results showed that in the presence of $Mg^{2+}$, tRSA could be revealed by streptavidin-DAB within a very short time (approximately 20 s), while color development for too long could dramatically increase the false positive hits. However, because of the interference from endogenous biotin, we argued that if this method was utilized in the transgenic animal model, *in situ* hybridization specific for the streptavidin aptamer sequence should be performed with the methods described previously [17].

In summary, our study has shown that the tRSA tag can be applied for identifying direct miRNA–mRNA interactions *in vitro* and that this tag can be revealed with a simple staining method. Additionally, all the aforementioned advantages could make the *in vivo* high-throughput identification of miRNAs binding to a specific target RNA sequence as simple as ChIP-sequencing.

## Acknowledgments

The authors deny any conflicts of interest related to this study. This work was supported by grants from the National Natural Science Foundation of China (81070797) and the National 973 project of China (2010CB534915).

## Appendix A. Supplementary data

Supplementary data associated with this article can be found, in the online version, at http://dx.doi.org/10.1016/j.bbrc.2012.05.002.

## References

[1] S. Istrail, E.H. Davidson, Logic functions of the genomic cis-regulatory code, Proc. Nat. Acad. Sci. USA 102 (2005) 4954–4959.
[2] L. He, G.J. Hannon, MicroRNAs: small RNAs with a big role in gene regulation, Nature Rev. Genet. 5 (2004) 522–531.
[3] D.P. Bartel, MicroRNAs: target recognition and regulatory functions, Cell 136 (2009) 215–233.
[4] K.N. Ivey, D. Srivastava, MicroRNAs as regulators of differentiation and cell fate decisions, Cell Stem Cell 7 (2010) 36–41.
[5] K.C. Miranda, T. Huynh, Y. Tay, Y.-S. Ang, W.-L. Tam, A.M. Thomson, B. Lim, I. Rigoutsos, A pattern-based method for the identification of microrna binding sites and their corresponding heteroduplexes, Cell 126 (2006) 1203–1217.
[6] G. Easow, A.A. Teleman, S.M. Cohen, Isolation of microRNA targets by miRNP immunopurification, RNA 13 (2007) 1198–1204.
[7] J.D. Keene, J.M. Komisarow, M.B. Friedersdorf, RIP-Chip: the isolation and identification of mRNAs, microRNAs and protein components of ribonucleoprotein complexes from cell extracts, Nat. Protocols 1 (2006) 302–307.
[8] S.W. Chi, J.B. Zang, A. Mele, R.B. Darnell, Argonaute HITS-CLIP decodes microRNA–mRNA interaction maps, Nature 460 (2009) 479–486.

[9] M. Hafner, M. Landthaler, L. Burger, M. Khorshid, J. Hausser, P. Berninger, A. Rothballer, M. Ascano, A.-C. Jungkamp, M. Munschauer, A. Ulrich, G.S. Wardle, S. Dewell, M. Zavolan, T. Tuschl, Transcriptome-wide identification of RNA-binding protein and microRNA target sites by PAR-CLIP, Cell 141 (2010) 129–141.
[10] U.A. Ørom, A.H. Lund, Isolation of microRNA targets using biotinylated synthetic microRNAs, Methods 43 (2007) 162–165.
[11] C. Srisawat, D.R. Engelke, Streptavidin aptamers: affinity tags for the study of RNAs and ribonucleoproteins, RNA 7 (2001) 632–641.
[12] H. Iioka, D. Loiselle, T.A. Haystead, I.G. Macara, Efficient detection of RNA–protein interactions using tethered RNAs, Nucleic Acids Res. 39 (2011) e53.
[13] P.F. Agris, The importance of being modified: roles of modified nucleosides and $Mg^{2+}$ in RNA structure and function, Prog. Nucleic Acid Res. Mol. Biol. 53 (1996) 79–129.
[14] L.A. Wu, J. Feng, L. Wang, Y.D. Mu, A. Baker, K.J. Donly, J. Gluhak-Heinrich, S.E. Harris, M. MacDougall, S. Chen, Immortalized mouse floxed Bmp2 dental papilla mesenchymal cell lines preserve odontoblastic phenotype and respond to BMP2, J. Cell Physiol. 225 (2010) 132–139.
[15] M.S. Ebert, J.R. Neilson, P.A. Sharp, MicroRNA sponges: competitive inhibitors of small RNAs in mammalian cells, Nat. Meth. 4 (2007) 721–726.
[16] P. Salmon, J. Oberholzer, T. Occhiodoro, P. Morel, J. Lou, D. Trono, Reversible immortalization of human primary cells by lentivector-mediated transfer of specific genes, Mol. Ther. 2 (2000) 404–414.
[17] S.C. Walker, P.D. Good, T.A. Gipson, D.R. Engelke, The Dual Use of RNA Aptamer Sequences for Affinity Purification and Localization Studies of RNAs and RNA–Protein Complexes RNA Detection and Visualization, in: J.E. Gerst (ed.), Humana Press, 2011, pp. 423–444.